LOW-COMPLEXITY MINIMUM-SER CHANNEL EQUALIZATION FOR OFDM UNDERWATER ACOUSTIC COMMUNICATIONS

Beixiong Zheng, Fangjiong Chen, Miaowen Wen, Fei Ji, and Hua Yu

School of Electronic and Information Engineering,
South China University of Technology, Guangzhou 510641, China

ABSTRACT

Orthogonal frequency division multiplexing (OFDM) is promising for underwater acoustic (UWA) communications as it is robust against large delay spread. However, OFDM suffers from intercarrier interference (ICI) caused by the serious Doppler effect in UWA channels. Attentive to the property that the ICI is mainly contributed by the adjacent subcarriers in UWA channels, in this paper, we propose a novel low-complexity frequency-domain equalizer to combat the ICI for OFDM UWA communications. Specifically, the coefficients of the equalizer are obtained by using the normalized gradient algorithm which is based on the minimum symbol error rate (MSER) criterion. The proposed equalizer uses very few (typical 3) FIR taps to mitigate the ICI for each subchannel, yet achieves better SER performance than the conventional equalizer based on the minimum mean square error (MMSE) criterion.

***Index Terms*—** Minimum-symbol-error rate, intercarrier interference (ICI), orthogonal frequency division multiplexing (OFDM), underwater acoustic communications.

1. INTRODUCTION

OFDM has high spectrum efficiency and significantly reduces the complexity of the equalization by converting the frequency-selective fading channel into several parallel flat fading channels. Due to the advantages it promises, OFDM prevails in various applications, such as wireless local area networks (WLAN), digital multimedia broadcasting (DMB), and UWA communications [1, 2]. However, OFDM systems are very vulnerable to the frequency offset, especially for UWA channels, where the Doppler effect is severe due to ocean waves and the transceiver motion. The frequency offset is very harmful since it gives rise to ICI, which significantly deteriorates the system performance. To mitigate the ICI, many ICI countermeasures have been proposed for OFDM UWA communications [3, 4]. Compared with the others, frequency-domain equalization attracts much more attention for its simplicity and effectiveness [5].

This work was supported by the NSFC (No.61322108, 61171083, 61431005, 61372083), the Key Grant Project of Chinese Ministry of Education (No.313021), the NCET program (No. NCET-12-0196), and Guangdong Provincial research project (No.2012B091100138).

The conventional MMSE-based equalizer requires an $N \times N$ matrix inversion with N being the total number of OFDM subcarriers, leading to $O\left(N^3\right)$ computational complexity. It becomes impractical for OFDM UWA communications in which N is usually very large, e.g., $N = 1024$, due to the large delay spread. Recently, by virtue of the property that in UWA channels the ICI mainly concentrates on the neighboring subcarriers [6, 7, 8], and the frequency-domain channel matrix (FCM) can be approximated as a banded matrix, serial equalizers of lower complexity are proposed in [9, 10, 11]. Those equalizers are designed based on the MMSE criterion, which intends to minimize the mean square error (MSE) between the equalizer output and the target signal. However, various simulations and analysis have illustrated that minimizing the MSE does not necessarily achieve the minimum of SER [12, 13, 14], which is desirable for UWA communications where the SER is high due to the severe ICI. Attentive to this, more recently, attention has been turned to the design of equalizers based on the MSER criterion [12, 13, 15, 16]. Nevertheless, those equalizers are only applicable to single carrier systems in the time domain.

To fill the aforementioned gap, in this paper, we design a low-complexity MSER-based frequency-domain equalizer to reduce the ICI for OFDM UWA communication systems by resorting to the banded structure of the FCM. Specifically, the proposed equalizer first converts the banded FCM into a tridiagonal matrix and divides the tridiagonal matrix into N submatrices for N subcarriers. Then, the SER expression after equalization and the update equation based on MSER are derived for systems with QAM modulation. We show that on one hand, the proposed equalizer with very few taps performs much better than the existing equalizers in terms of the SER for OFDM UWA communications, and on the other hand, the proposed equalization can be computed in parallel and independently for each subcarrier, significantly saving the computational time and complexity.

2. SYSTEM MODEL

2.1. OFDM signal model

We consider an OFDM system with N subcarriers, where N is a power of 2. Denote an OFDM symbol block including

N baseband symbols as $\mathbf{X} = [X_1, ..., X_N]^T$. Using the N-point inverse discrete Fourier transform (IDFT) to convert the OFDM symbol $\mathbf{X}$ into time-domain signal block $\mathbf{x}$ gives

$$\mathbf{x} = \mathbf{F}^H \mathbf{X}, \tag{1}$$

where $\mathbf{F}$ is the $N \times N$ unitary normalized discrete Fourier transform (DFT) matrix, defined by $[\mathbf{F}]_{\imath,\jmath} = \frac{1}{\sqrt{N}} e^{-j2\pi\imath\jmath/N}$ with $0 \leq \imath, \jmath \leq N-1$.

To eliminate the intersymbol interference (ISI) between adjacent OFDM symbols, the cyclic prefix (CP) is appended to the beginning of an OFDM symbol. After a travel through the channel and the removal of the CP, the received signal block in the time domain is given by

$$\mathbf{y} = \mathbf{H}\mathbf{x} + \mathbf{v}, \tag{2}$$

where $\mathbf{v}$ is the time-domain noise vector and $\mathbf{H}$ is the time-domain channel matrix (TCM). Here, the element of $\mathbf{H}$ is given by $[\mathbf{H}]_{k,l} = h(k, \langle k-l \rangle_N)$[1], where k and l denote the time index and the lag, respectively.

After applying the N-point DFT to (2), the received signal bolck in the frequency domain can be expressed as

$$\mathbf{Y} = \mathbf{F}\mathbf{y} = \mathbf{F}\mathbf{H}\mathbf{F}^H\mathbf{X} + \mathbf{F}\mathbf{v} = \mathbf{G}\mathbf{X} + \mathbf{V}, \tag{3}$$

where $\mathbf{G} = \mathbf{F}\mathbf{H}\mathbf{F}^H$ denotes the $N \times N$ frequency-domain channel matrix and $\mathbf{V} = \mathbf{F}\mathbf{v}$ is the frequency-domain noise vector.

For time-invariant channels, the time-domain channel matrix $\mathbf{H}$ is a circulant matrix and the corresponding frequency-domain channel matrix $\mathbf{G}$ is a diagonal matrix. In this case, there is no ICI and the decoding can be realized easily by one-tap equalization. However, when the channel is time-varying due to the Doppler spread, the subcarriers are no longer orthogonal and ICI arises.

2.2. Banded structure of the FCM

It is well known that the Doppler frequencies not only depend on the carrier frequency f_c and the relative motion v, but also on the speed of signal wave propagation c and the scattering environment [17]. Since it is $c = 3 \times 10^8 m/s$ for the electromagnetic wave, while $c \approx 1500 m/s$ for the UWA wave, the Doppler effect is more significant in UWA communications than that in wireless radio communications.

As analyzed above, the frequency-domain channel matrix $\mathbf{G}$ is not diagonal in OFDM UWA communications. Since it is shown in [6, Fig. 10] by the UWA experiment that the ICI between two subcarriers decreases rapidly as their separation increases and the ICI power mainly centers on the two closest subcarriers, $\mathbf{G}$ can be well approximated as a banded matrix $\hat{\mathbf{G}}$ [7], as illustrated in Fig. 1. The banded matrix is composed of a $2D+1$ main diagonal matrix and two $D \times D$ triangular matrices. The width of the banded matrix can be regarded as the range of the ICI.

[1] $\langle k \rangle_N$ denotes k mod N.

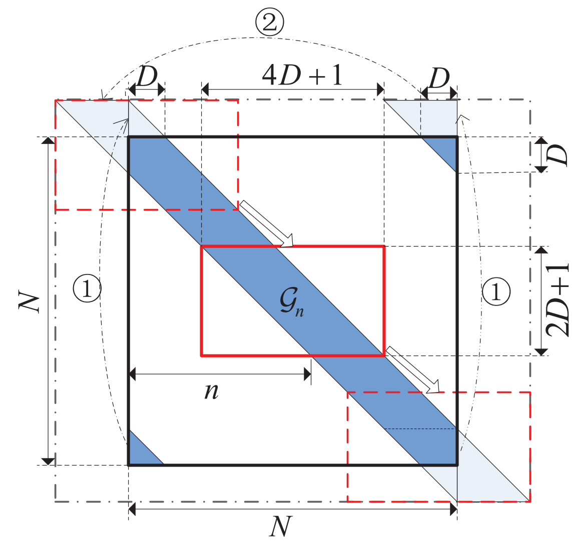

Fig. 1. Banded structure of FCM and its decomposition.

As the ICI is mainly contributed by the two immediate neighbors (the first and last subcarriers can be regarded as adjacent subcarriers), we have $D = 1$. Furthermore, when the Doppler effect becomes more severe, the windowing scheme [18, 19] can be applied to control the ICI power in the desired short range, which in turn confines the ICI effect within a limited number of neighboring subcarriers. The restriction $D = 1$ for the banded matrix $\hat{\mathbf{G}}$ makes it suitable for the design of the equalizer with few (typical $2D+1 = 3$) FIR taps to mitigate the ICI.

3. DECOMPOSITION OF FCM AND EQUALIZATION

The output of the 3-tap equalizer for the estimation of the nth subcarrier can be derived as

$$\hat{X}_n = \mathbf{c}_n^T \mathbf{Y}_n \doteq \mathbf{c}_n^T \mathcal{G}_n \mathbf{X}_n + V_n, \tag{4}$$

where $\mathbf{Y}_n = [Y_{\langle n-1 \rangle_N}, Y_{\langle n \rangle_N}, Y_{\langle n+1 \rangle_N}]^T$, $V_n = \mathbf{c}_n^T \mathbf{V}_n$, $\mathbf{X}_n = [X_{\langle n-2 \rangle_N}, X_{\langle n-1 \rangle_N}, X_{\langle n \rangle_N}, X_{\langle n+1 \rangle_N}, X_{\langle n+2 \rangle_N}]^T$, and

$$\mathcal{G}_n = \begin{bmatrix} [\hat{\mathbf{G}}]_{\langle n-1 \rangle_N, \langle n-2 \rangle_N} & \cdots & [\hat{\mathbf{G}}]_{\langle n-1 \rangle_N, \langle n+2 \rangle_N} \\ [\hat{\mathbf{G}}]_{\langle n \rangle_N, \langle n-2 \rangle_N} & \cdots & [\hat{\mathbf{G}}]_{\langle n \rangle_N, \langle n+2 \rangle_N} \\ [\hat{\mathbf{G}}]_{\langle n+1 \rangle_N, \langle n-2 \rangle_N} & \cdots & [\hat{\mathbf{G}}]_{\langle n+1 \rangle_N, \langle n+2 \rangle_N} \end{bmatrix}. \tag{5}$$

Here, $\mathcal{G}_n$ denotes the submatrix for the nth subcarrier, which is obtained by using a 3×5 mask operated on the banded matrix $\hat{\mathbf{G}}$. Fig. 1 shows the mask marked as a red rectangular box, which is slid on the diagonal direction of $\hat{\mathbf{G}}$. However, the mask will lie outside $\hat{\mathbf{G}}$ for the first and last submatrices. To solve this problem, the banded matrix $\hat{\mathbf{G}}$ is extended to a

$(N+2)\times(N+4)$ tridiagonal matrix, as shown in Fig. 1. The extension can be described in the following steps:

① For the first submatrix, copy the last row of the banded matrix $\hat{\mathbf{G}}$, and then add it to the top of the matrix;

② Copy the 2×2 triangular matrix in the top-right corner, and then add it to the the top-left corner of the new matrix;

③ For the last submatrix, do the similar operations to steps ① and ②.

According to (4), a 3-tap equalizer [9] based on the MMSE criterion is given by

$$\mathbf{c}_n^T = \mathbf{e}^T \mathcal{G}_n^H (\mathcal{G}_n \mathcal{G}_n^H + \sigma^2 \mathbf{I})^{-1}, \tag{6}$$

where $\mathbf{e} = [0,0,1,0,0]^T$. Since the equalization of the whole OFDM symbol using an $N\times N$ matrix inversion is impractical for a large N, the equalization of (6) can reduce the complexity significantly [9]. However, the reduction of complexity comes at the cost of SER performance, which means that the equalizer based on the MMSE criterion in (6) is suboptimal in the sense of SER performance. In the next section, we will propose an equalizer based on the MSER criterion, which improves the SER performance without increasing the number of taps required in (6).

4. UPDATE EQUATION BASED ON THE MSER

For analytical simplicity, we assume that the receiver has an accurate estimate of the banded part coefficients of the frequency-domain channel, i.e., the banded matrix $\hat{\mathbf{G}}$ is perfectly known, following [19].

4.1. SER for QAM source

In this work, the discussion for BPSK source in [13] is extended to QAM source. The modulated symbol carried on a subcarrier is composed of two independent PAM symbols, which can be written as

$$X_n = X_n^R + j\cdot X_n^I, \tag{7}$$

where $(\cdot)^R$ and $(\cdot)^I$ denote the real and imaginary parts, respectively. Consider the 4-QAM modulation, and the power spectral density of complex noise $\mathbf{V}_n$ in (4) is $2\sigma^2$. After equalization of (4) and the optimal detection [20, Section 4.1] based on Gaussian channels, we can obtain the following SER after some derivations:

$$\begin{aligned}\mathrm{SER} = P_e &= \frac{1}{2}P_e^R + \frac{1}{2}P_e^I \\ &= \frac{1}{2}\left(E\left[Q\left(\frac{(\mathbf{c}_n^T\hat{\mathbf{S}})^R}{\|\mathbf{c}_n\|\sigma}\right)\right] + E\left[Q\left(\frac{(\mathbf{c}_n^T\check{\mathbf{S}})^I}{\|\mathbf{c}_n\|\sigma}\right)\right]\right),\end{aligned} \tag{8}$$

where $Q(\cdot)$ is the Gaussian Q-function, $\hat{\mathbf{S}} = \mathcal{G}_n\mathbf{X}_n X_n^R$, and $\check{\mathbf{S}} = \mathcal{G}_n\mathbf{X}_n X_n^I$. Here, $\hat{\mathbf{S}}$ is a random vector with distribution $P(\hat{\mathbf{S}}) = P(\mathbf{X}\,|X_n^R = 1)$, while $\check{\mathbf{S}}$ is a random vector with distribution $P(\check{\mathbf{S}}) = P(\mathbf{X}\,|X_n^I = 1)$. The modulated symbols are assumed to be distributed uniformly and independently, so that $\hat{\mathbf{S}}$ and $\check{\mathbf{S}}$ follow uniform distribution. Based on the distributions of $\hat{\mathbf{S}}$ and $\check{\mathbf{S}}$, we have $P(\check{\mathbf{S}}) = P(j\cdot\hat{\mathbf{S}})$ and

$$E\left[Q\left(\frac{(\mathbf{c}_n^T\check{\mathbf{S}})^I}{\|\mathbf{c}_n\|\sigma}\right)\right] = E\left[Q\left(\frac{(j\cdot\mathbf{c}_n^T\hat{\mathbf{S}})^I}{\|\mathbf{c}_n\|\sigma}\right)\right] = E\left[Q\left(\frac{(\mathbf{c}_n^T\hat{\mathbf{S}})^R}{\|\mathbf{c}_n\|\sigma}\right)\right]. \tag{9}$$

Then substituting (9) into (8) yields

$$\mathrm{SER} = E\left[Q\left(\frac{(\mathbf{c}_n^T\hat{\mathbf{S}})^R}{\|\mathbf{c}_n\|\sigma}\right)\right] = \frac{1}{K}\sum_{k=1}^{K} Q\left(\frac{(\mathbf{c}_n^T\hat{\mathbf{S}}_{(k)})^R}{\|\mathbf{c}_n\|\sigma}\right), \tag{10}$$

where $K = 2\times 4^4$ denotes the number of all possible cases of $\hat{\mathbf{S}}_{(k)}$. Convert the complex vectors into the real vectors as $\bar{\mathbf{c}}_n = [\mathbf{c}_n^R; -\mathbf{c}_n^I]$ and $\bar{\hat{\mathbf{S}}}_{(k)} = [\hat{\mathbf{S}}_{(k)}^R; \hat{\mathbf{S}}_{(k)}^I]$. Then (10) can be simplified as

$$\mathrm{SER} = \frac{1}{K}\sum_{k=1}^{K} Q\left(\frac{\bar{\mathbf{c}}_n^T\bar{\hat{\mathbf{S}}}_{(k)}}{\|\bar{\mathbf{c}}_n\|\sigma}\right). \tag{11}$$

Recall that $\|\bar{\mathbf{c}}_n\| = \|\mathbf{c}_n\|$. The gradient of the SER in (11) with respect to $\bar{\mathbf{c}}_n$ is

$$\nabla_{\bar{\mathbf{c}}}\mathrm{SER} = \frac{-1}{\sqrt{2\pi}\sigma\,\|\bar{\mathbf{c}}_n\|}\left(\mathbf{I} - \frac{\bar{\mathbf{c}}_n\bar{\mathbf{c}}_n^T}{\|\bar{\mathbf{c}}_n\|^2}\right) f(\bar{\mathbf{c}}_n), \tag{12}$$

where

$$f(\bar{\mathbf{c}}_n) = \frac{1}{K}\sum_{k=1}^{K} e^{-u_k^2/2}\bar{\hat{\mathbf{S}}}_{(k)}, \tag{13}$$

in which u_k is the real part of one normalized equalization output of different received signals:

$$u_k = \frac{\bar{\mathbf{c}}_n^T\bar{\hat{\mathbf{S}}}_{(k)}}{\|\bar{\mathbf{c}}_n\|\sigma} = \frac{(\mathbf{c}_n^T\hat{\mathbf{S}}_{(k)})^R}{\|\mathbf{c}_n\|\sigma}. \tag{14}$$

4.2. Update equation

As it is very difficult to obtain the closed-form solution to satisfy $\nabla_{\bar{\mathbf{c}}}\mathrm{SER} = 0$, here we develop a gradient algorithm to search for the minima. The normalized gradient algorithm based on (12) is given by

$$\begin{aligned}\bar{\mathbf{c}}_{n,i+1} &= \bar{\mathbf{c}}_{n,i} - \mu_n\sqrt{2\pi}\sigma\,\|\bar{\mathbf{c}}_{n,i}\|\cdot\nabla_{\bar{\mathbf{c}}_{n,i}}\mathrm{SER} \\ &= \bar{\mathbf{c}}_{n,i} - \mu_n\left(\mathbf{I} - \frac{\bar{\mathbf{c}}_{n,i}\bar{\mathbf{c}}_{n,i}^T}{\|\bar{\mathbf{c}}_{n,i}\|^2}\right) f(\bar{\mathbf{c}}_{n,i}) \\ &= \left(1 - \mu_n\bar{\mathbf{c}}_{n,i}^T f(\bar{\mathbf{c}}_{n,i})/\|\bar{\mathbf{c}}_{n,i}\|^2\right)\left(\bar{\mathbf{c}}_{n,i} + \mu f(\bar{\mathbf{c}}_{n,i})\right),\end{aligned} \tag{15}$$

where subscript i denotes the update time and $\mu = \mu_n/(1 - \mu_n\bar{\mathbf{c}}_{n,i}^T f(\bar{\mathbf{c}}_{n,i})/\|\bar{\mathbf{c}}_{n,i}\|^2)$. It is worth mentioning that the norm of $\bar{\mathbf{c}}_n$ has no impact on the SER in (11) and the factor $\left(1 - \mu_n\bar{\mathbf{c}}_{n,i}^T f(\bar{\mathbf{c}}_{n,i})/\|\bar{\mathbf{c}}_{n,i}\|^2\right)$ works just as an coefficient of the norm of $\bar{\mathbf{c}}_{n,i+1}$. After removing this factor, we obtain the following update equation:

$$\bar{\mathbf{c}}_{n,i+1} = \bar{\mathbf{c}}_{n,i} + \mu f(\bar{\mathbf{c}}_{n,i}). \quad (16)$$

We revert back to $\mathbf{c}_n$ by applying a permutation matrix:

$$\mathbf{c}_n = \mathbf{c}_n^R + j \cdot \mathbf{c}_n^I = \mathbf{P}\bar{\mathbf{c}}_n, \quad (17)$$

where $\mathbf{P} = [\mathbf{I}, -j\mathbf{I}]$ is a permutation matrix of size 3×6. Then, left multiplying the update equation (16) by the permutation matrix, we obtain the following update equation for QAM source:

$$\mathbf{c}_{n,i+1} = \mathbf{c}_{n,i} + \mu \frac{1}{K} \sum_{k=1}^{K} e^{-u_k^2/2} \hat{\mathbf{S}}_{(k)}^{*}, \quad (18)$$

where $(\cdot)^*$ denotes the conjugation operation.

Due to the non-convex property of the SER surface, the gradient algorithm may not converge to the global extremum. Hence, a good initial condition is important for the update equation in (18). The simulations will show that it is an effective way to choose the MMSE-based equalizer (6) as the initial condition for the update equation (18).

5. SIMULATION RESULTS AND ANALYSIS

In this section, we consider an OFDM system with 4-QAM modulation in the UWA channel simulator of [7, 21]. The number of subcarriers is set to be $N = 1024$, $N_{CP} = 256$, and the bandwidth of the UWA channel is 10kHz at the center frequency of 15kHz.

To investigate the the performance of the equalizers under the high adjacent ICI scenario, first we exploit the performance of the proposed equalizer for the frequency-domain channel matrix $\mathbf{G}$ with strictly banded structure. The ratio of left adjacent ICI power to the detected subcarriers power is set to be 0.9, the ratio of right adjacent ICI power to the detected subcarriers power is set to be 0.4, and the frequency channel coefficients are generated by Gaussian process independently. Fig. 2 compares the SER performance of the equalizers in terms of SER versus signal-to-noise ratio (SNR). It can be observed that the one-tap equalizer is less efficient under the high adjacent ICI scenario, and the 3-tap equalizer based on the MMSE criterion is much better in the ICI reduction. Note that the 3-tap equalizer based on the MSER criterion exhibits the best performance among the equalizers, especially at high SNR.

Fig. 3 shows the SER versus the SNR for different equalizers in doubly-selective UWA channels with the normalized Doppler shift equal to 0.6. As the frequency-domain channel matrix $\mathbf{G}$ is not strictly banded when UWA channels suffer from severe Doppler effect, the interference of non-adjacent subcarriers can not be ignored. Then the banded approximation of $\mathbf{G}$ may have some deviations. As a result, the SER of the system is relatively high. However, the 3-tap equalizer based on the MSER criterion still performs better than the equalizer based on the MMSE criterion, showing its superiority in UWA communications.

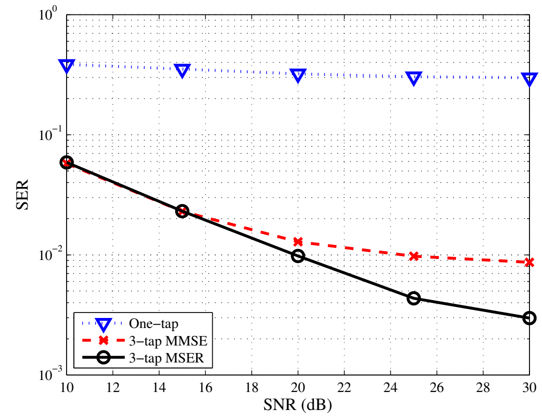

Fig. 2. SER comparison of different equalizations in OFDM systems with strictly banded FCM.

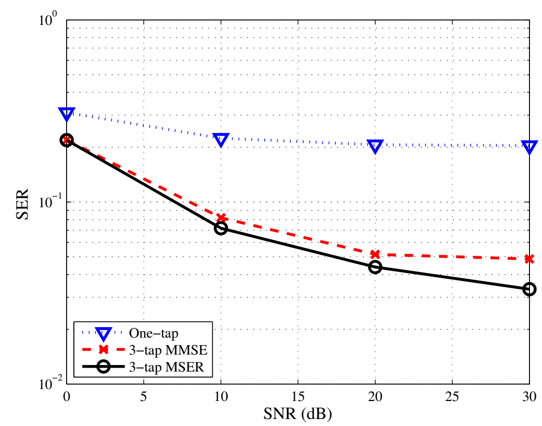

Fig. 3. SER comparison of different equalizations in OFDM systems over UWA channels with approximated-banded FCM.

6. CONCLUSION

In this work, we have proposed a low-complexity equalizer based on the MSER criterion to mitigate the ICI due to the Doppler effect. Compared with the widely adopted MMSE-based equalizer, the proposed equalizer achieves much better SER performance while keeps the same number of equalization taps. Moreover, the proposed equalizer will have more benefits on the SER performance when more ICI energy concentrates on the neighboring subcarriers. As the SER of an UWA communication system is relatively high, a lower SER is very demanding. In this sense, the proposed equalizer is more favorable for OFDM UWA communications.

7. REFERENCES

[1] H. Hijazi and L. Ros, "Joint data QR-detection and Kalman estimation for OFDM time-varying Rayleigh channel complex gains," *IEEE Transactions on Communications*, vol. 58, no. 1, pp. 170–178, Jan. 2010.

[2] M. Stojanovic, "Underwater acoustic communications: Design considerations on the physical layer," in *Proceedings of IEEE/IFIP Fifth Annual Conference on Wireless on Demand Network Systems and Services*, Garmisch-Partenkirchen, Germany, Jan. 2008, pp. 1–10.

[3] C. R. Berger, S. Zhou, *et al.*, "Sparse Channel Estimation for Multicarrier Underwater Acoustic Communication: From Subspace Methods to Compressed Sensing,"*IEEE Transactions on Signal Processing*, vol. 58, no. 3, pp. 1708–1721, Mar. 2010.

[4] A. Ancora, G. Montalbano, and DTM. Slock, "Preconditioned iterative inter-carrier interference cancellation for OFDM reception in rapidly varying channels," in *Proceedings of 2010 IEEE International Conference on Acoustics Speech and Signal Processing (ICASSP)*, Dallas, TX, USA, Mar. 2010, pp. 3066–3069.

[5] E. Panayirci, H. Senol, and H. V. Poor, "Joint channel estimation, equalization, and data detection for OFDM systems in the presence of very high mobility," *IEEE Transactions on Signal Processing*, vol. 58, no. 8, pp. 4225–4238, Aug. 2010.

[6] K. Tu, D. Fertonani, *et al.*, "Mitigation of intercarrier interference for OFDM over time-varying underwater acoustic channels," *IEEE Journal of Oceanic Engineering*, vol. 36, no. 2, pp. 156–171, April 2011.

[7] H. Yu, A. Song, *et al.*, "Iterative estimation of the time-varying underwater acoustic channel using basis expansion models," in *Proceedings of the Eighth ACM International Conference on Underwater Networks and Systems*, Kaohsiung, Taiwan, Nov. 2013, pp. 1–8.

[8] J. -Z. Huang, S. Zhou, *et al.*, "Progressive Inter-carrier Interference Equalization for OFDM Transmission over Time-varying Underwater Acoustic Channels," *IEEE Journal of Selected Topics in Signal Processing*, vol. 5, no. 8, pp. 1524–1536, Dec. 2011.

[9] S. Lu, R. Kalbasi, and N. Al-Dhahir, "OFDM interference mitigation algorithms for doubly-selective channels," in *Proceedings of IEEE 64th Vehicular Technology Conference*, Montreal, Canada, Sept. 2006, pp. 1–5.

[10] B. Narasimhan, D. Wang, *et al.*, "Digital compensation of frequency-dependent joint Tx/Rx I/Q imbalance in OFDM systems under high mobility," *IEEE Journal of Selected Topics in Signal Processing*, vol. 3, no. 3, pp. 405–417, June 2009

[11] S. Lu and N. Al-Dhahir, "Coherent and differential ICI cancellation for mobile OFDM with application to DVB-H," *IEEE Transactions on Wireless Communications*, vol. 7, no. 11, pp. 4110–4116, Nov. 2008

[12] C. -C. Yeh and J. R. Barry, "Adaptive minimum symbol-error rate equalization for quadrature-amplitude modulation," *IEEE Transactions on Signal Processing*, vol. 51, no. 12, pp. 3263–3269, Dec. 2003.

[13] C. -C. Yeh and J. R. Barry, "Adaptive minimum bit-error rate equalization for binary signaling," *IEEE Transactions on Communications*, vol. 48, no. 7, pp. 1226–1235, July 2000.

[14] S. Chen, S. Tan, *et al.*, "Adaptive minimum error-rate filtering design: A review," *Signal Processing*, vol. 88, no. 7, pp. 1671–1697, July 2008.

[15] M. Gong, F. Chen, *et al.*, "Normalized adaptive channel equalizer based on minimal symbol-error-rate," *IEEE Transactions on Communications*, vol. 61, no. 4, pp. 1374–1383, April 2013.

[16] B. Zheng, F. Chen, *et al.*, "Least-symbol-error-rate adaptive decision feedback equalization for underwater channel," in *Proceedings of the Eighth ACM International Conference on Underwater Networks and Systems*, Kaohsiung, Taiwan, Nov. 2013, pp. 1–5.

[17] T. Zemen and C. F. Mecklenbrauker, "Time-variant channel estimation using discrete prolate spheroidal sequences," *IEEE Transactions on Signal Processing*, vol. 53, no. 9, pp. 3597–3607, Sept. 2005.

[18] P. Schniter and S. D'Silva, "Low-complexity detection of OFDM in doubly-dispersive channels," in *Proceedings of Asilomar Conference on Signals, Systems and Computers*, Pacific Grove, CA, USA, Nov. 2002, pp. 1799–1803.

[19] A. A. Abotabl, A. El-Keyi, *et al.*, "Optimal windowing and decision feedback equalization for space-frequency Alamouti-coded OFDM in doubly selective channels," *IEEE Transactions on Vehicular Technology*, vol. 63, no. 5, pp. 2197–2207, June 2014.

[20] J. G. Proakis, *Digital Communications*, 5th ed. New York: McGraw Hill, 2007.

[21] A. Song, J. Senne, *et al.*, "Underwater acoustic communication channel simulation using parabolic equation," in *Proceedings of the Sixth ACM International Workshop on Underwater Networks*, Seattle, WA, USA, Dec. 2011, pp. 1–5.